PHOTONICS Research

Nonreciprocal unconventional photon blockade in a spinning optomechanical system

Baijun Li,[1] Ran Huang,[1] Xunwei Xu,[2] Adam Miranowicz,[3,4,5] and Hui Jing[1,6]

[1]Key Laboratory of Low-Dimensional Quantum Structures and Quantum Control of Ministry of Education, Department of Physics and Synergetic Innovation Center for Quantum Effects and Applications, Hunan Normal University, Changsha 410081, China
[2]Department of Applied Physics, East China Jiaotong University, Nanchang 330013, China
[3]Theoretical Quantum Physics Laboratory, RIKEN Cluster for Pioneering Research, Wako-shi, Saitama 351-0198, Japan
[4]Faculty of Physics, Adam Mickiewicz University, 61-614 Poznan, Poland
[5]e-mail: miran@amu.edu.pl
[6]e-mail: jinghui73@gmail.com

Received 1 February 2019; revised 19 March 2019; accepted 19 March 2019; posted 20 March 2019 (Doc. ID 359390); published 14 May 2019

We propose how to achieve quantum nonreciprocity via unconventional photon blockade (UPB) in a compound device consisting of an optical harmonic resonator and a spinning optomechanical resonator. We show that, even with very weak single-photon nonlinearity, nonreciprocal UPB can emerge in this system, i.e., strong photon antibunching can emerge only by driving the device from one side but not from the other side. This nonreciprocity results from the Fizeau drag, leading to different splitting of the resonance frequencies for the optical counter-circulating modes. Such quantum nonreciprocal devices can be particularly useful in achieving back-action-free quantum sensing or chiral photonic communications.

https://doi.org/10.1364/PRJ.7.000630

1. INTRODUCTION

Photon blockade (PB) [1–5], i.e., the generation of the first photon in a nonlinear cavity, diminishes to almost zero the probability of generating another photon in the cavity; it plays a key role in single-photon control for quantum technology applications nowadays [6–8]. In experiments, PB has been demonstrated in cavity-QED or circuit-QED systems [4,5,9–12]. It has also been predicted in various nonlinear optical systems [13–15] and optomechanical (OM) devices [16–20]. Conventional PB occurs under the stringent condition of strong single-photon nonlinearities, which is highly challenging in practice.

To overcome this obstacle, coupled-resonator systems, with destructive interferences of different dissipative pathways [21–24], have been proposed to achieve unconventional PB (UPB) even for arbitrarily weak nonlinearities [23–37]. UPB provides a powerful tool to generate optimally sub-Poissonian light and also a way to reveal quantum correlations in weakly nonlinear devices [33,34]. Recently, UPB was demonstrated experimentally in coupled optical [36] or superconducting resonators [37].

It should be stressed that PB and UPB are very different phenomena, and, thus, their nonreciprocal generalizations are different as well. Indeed PB refers to a process where a single photon is blocking the entry (or generation) of more photons in a strongly nonlinear cavity. Thus, PB refers to state truncation, also referred to as nonlinear quantum scissors [38,39]. PB can be used as a source of single photons, since the PB light is sub-Poissonian (or photon antibunched) in second and higher orders, as characterized by the correlation functions $g^{(n)}(0) < 1$ for $n = 2, 3, \ldots$. By contrast to PB, UPB refers to the light that is optimally sub-Poissonian in the second order, $g^2(0) \approx 0$, and is generated in a weakly nonlinear system allowing multi-path interference (e.g., two linearly coupled cavities, when one of them is also weakly coupled to a two-level atom). Thus, PB and UPB are induced by different effects: PB due to a large system nonlinearity and UPB via multipath interference even assuming extremely weak system nonlinearity. Note that light generated via UPB can exhibit higher-order super-Poissonian photon-number statistics, $g^{(n)}(0) > 1$ for some $n > 2$. Thus, UPB is, in general, not a good source of single photons. This short comparison of PB and UPB indicates that the term UPB, as coined in Ref. [40] and now commonly accepted, is fundamentally different from PB, concerning their physical mechanisms and the properties of the light generated in them.

Here, we propose achieving and controlling nonreciprocal UPB with spinning devices. Nonreciprocal devices allow the flow of light from one side but block it from the other. Thus, such devices can be applied in noise-free quantum information signal processing and quantum communication for canceling interfering signals [41]. Nonreciprocal optical devices have been realized in OM devices [41–43], Kerr resonators [44–46], thermo systems [47–49], devices with temporal modulation [50,51], and non-Hermitian systems [52–54].

In a very recent experiment [55], 99.6% optical isolation was achieved in a spinning resonator based on the optical Sagnac effect. By using the spinning resonators, optomechanically induced transparency [56] and ultrasensitive nanoparticle sensing [57] have also been studied. However, these studies have mainly focused on the classical regimes, i.e., unidirectional control of transmission rates instead of quantum noises. We also note that in recent works, single-photon diodes [58–60], unidirectional quantum amplifiers [61–65], and one-way quantum routers [66] have been explored. In particular, nonreciprocal PB was predicted in a Kerr resonator [67] or a quadratic OM system [68], which, however, relies on the conventional condition of strong single-photon nonlinearity. These quantum nonreciprocal devices have potential applications for quantum control of light chiral and topological quantum technologies [69].

We also note that coupled-cavity systems have been studied extensively in experiments [37,70–72], providing a unique way to achieve not only UPB, but also phonon laser [72–76], slow light [77], and force sensing [70,71,78]. Here, we study nonreciprocal UPB in a coupled system with an optical harmonic cavity and a spinning OM resonator. We find that, by the spinning of an OM resonator, UPB can emerge nonreciprocally even with weak single-photon nonlinearity; that is, strongly antibunched photons can emerge only when the device is driven from one side but not the other side. Our work opens up a new route to engineer quantum chiral UPB devices, which can have practical applications in achieving, for example, photonic diodes or circulators, and nonreciprocal quantum communications at the few-photon level.

2. MODEL AND SOLUTIONS

We consider a compound system consisting of an optical harmonic resonator (with a resonance frequency ω_L of the cavity field and a decay rate of κ_L) and a spinning anharmonic resonator (with a resonance frequency ω_R of the cavity field and a decay rate of κ_R), as shown in Fig. 1. External light is coupled into and out of the resonator through a tapered fiber of frequency ω_d and these two whispering-gallery-mode resonators are evanescently coupled to each other with a coupling strength of J [79]. Note that the required strong Kerr nonlinearity, $K \approx 3\kappa$ (where κ is the cavity linewidth), in the previous proposal [67] is challenging for the current experiments. Here, we can use an experimentally feasible Kerr-nonlinear strength to realize nonreciprocal PB, i.e., $K \approx 0.04\kappa$ [37], which is two orders of magnitude smaller than that in the former work [67]. Weak Kerr couplings can be achieved in cavity-atom systems [80], magnon devices [81], and OM systems [82], on which we focus here. We consider a weak OM coupling strength ($g \approx 0.63\kappa$) in an auxiliary cavity that is well within the current experimental abilities [83–85]. In a spinning resonator, the refractive indices associated with the clockwise (+) and anticlockwise (−) optical modes are given as $n_\pm = n[1 \pm nv(n^{-2} - 1)/c]$, where $v = r\Omega$ is the tangential velocity with an angular velocity of Ω and radius r [55]. For light propagating in the spinning resonator, the optical mode experiences a Fizeau shift Δ_F [86], that is, $\omega_R \to \omega_R + \Delta_F$, with

$$\Delta_F = \pm \frac{nr\Omega\omega_R}{c}\left(1 - \frac{1}{n^2} - \frac{\lambda}{n}\frac{dn}{d\lambda}\right) = \pm\eta\Omega, \tag{1}$$

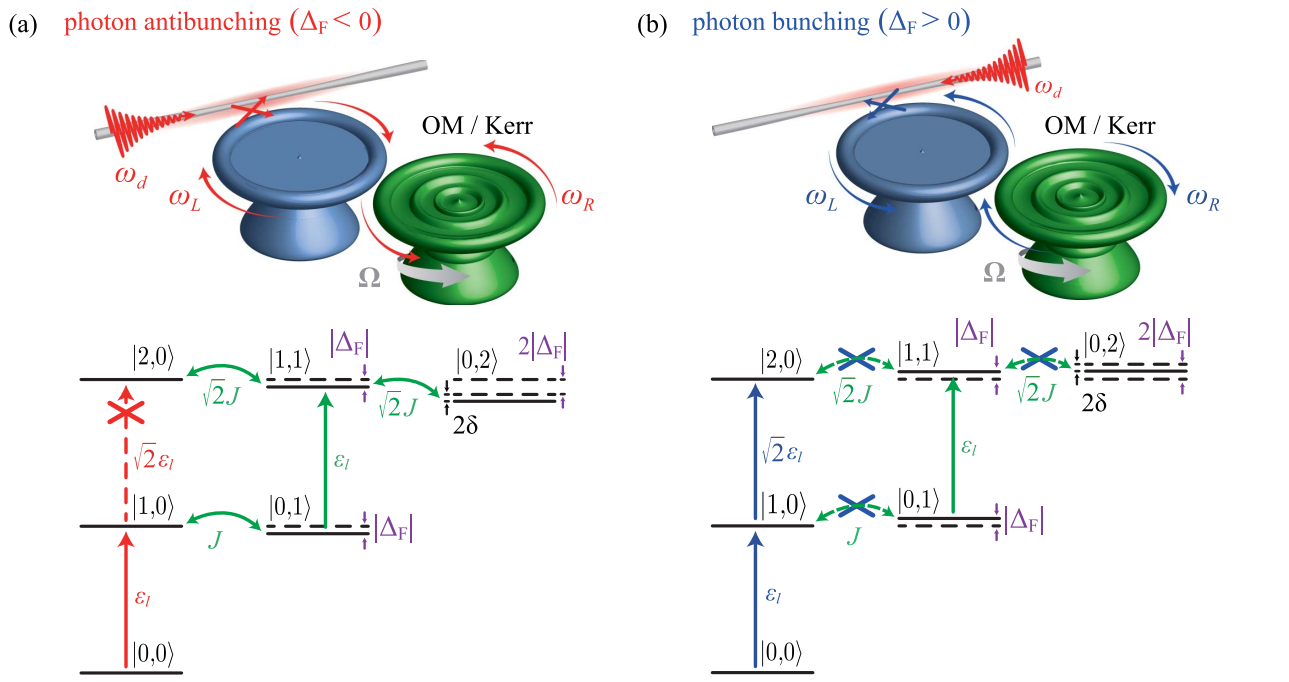

Fig. 1. Nonreciprocal UPB in a coupled-resonator system. Spinning the OM (Kerr-type) resonator results in different Fizeau drag Δ_F for the counter-circulating whispering-gallery modes of the resonator. (a) By driving the system from the left-hand side, the direct excitation from state $|1,0\rangle$ to state $|2,0\rangle$ (red dotted arrow) will be forbidden by destructive quantum interference with the other paths drawn by green arrows, leading to photon antibunching. (b) Photon bunching occurs when the system is driven from the right side, due to lack of complete destructive quantum interference between the indicated levels (drawn by crossed green dotted arrows). Here, $\delta = g^2/\omega_m$ is the energy shift induced by the OM nonlinearity.

where $\omega_R = 2\pi c/\lambda$ is the optical resonance frequency of the nonspinning OM resonator, c (λ) is the speed (wavelength) of light in vacuum, and n is the refractive index of the cavity. The dispersion term $dn/d\lambda$, characterizing the relativistic origin of the Sagnac effect, is relatively small in typical materials (~1%) [55,86]. For convenience, we always assume counterclockwise rotation of the resonator. Hence, $\pm\Delta_F$ denote light propagating against ($\Delta_F > 0$) and along ($\Delta_F < 0$) the direction of the spinning OM resonator, respectively.

In a rotating frame with respect to $H_0 = \omega_d(a_L^\dagger a_L + a_R^\dagger a_R)$, the effective Hamiltonian of the system can be written as (see Appendix A for more details)

$$\begin{aligned}\mathcal{H} &= \hbar\Delta_L a_L^\dagger a_L + \hbar(\Delta_R + \Delta_F)a_R^\dagger a_R + \hbar\omega_m b^\dagger b \\ &+ \hbar J(a_L^\dagger a_R + a_R^\dagger a_L) + \hbar g a_R^\dagger a_R(b^\dagger + b) \\ &+ i\hbar\epsilon_d(a_L^\dagger - a_L),\end{aligned} \tag{2}$$

where a_L ($a_L^\dagger$) and a_R ($a_R^\dagger$) are the photon annihilation (creation) operators for the cavity modes of the optical cavity (denoted with the subscript L) and the OM cavity (denoted with the subscript R), respectively. b ($b^\dagger$) is the annihilation (creation) operator for the mechanical mode of the OM cavity. The frequency detuning between the cavity field in the left (right) cavity and the driving field is denoted as $\Delta_K = \omega_K - \omega_d$, where $K = L, R$. The parameter J denotes the strength of the photon hopping interaction between the two cavity modes, and $g = \omega_R/r[\hbar/(2m\omega_m)]^{1/2}$ describes the radiation-pressure coupling between the optical and vibrative modes in the OM resonator with frequency ω_m and effective mass m. $\epsilon_d = \sqrt{\kappa_L P_{\rm in}/(\hbar\omega_d)}$ denotes the driving strength that is coupled into the compound system through the optical fiber waveguide with a cavity loss rate of κ_L and driving power $P_{\rm in}$.

The Heisenberg equations of motion of the system are then written as

$$\begin{aligned}\frac{d}{dt}q &= \omega_m p, \\ \frac{d}{dt}p &= -\omega_m q - g_b a_R^\dagger a_R - \frac{\gamma_m}{2}p + \xi, \\ \frac{d}{dt}a_L &= -\left(\frac{\kappa_L}{2} + i\Delta_L\right)a_L - iJa_R + \epsilon_d + \sqrt{\kappa_L}a_{L,\rm in}, \\ \frac{d}{dt}a_R &= -\left(\frac{\kappa_R}{2} + i\Delta_R'\right)a_R - iJa_L - ig_b q a_R + \sqrt{\kappa_L}a_{R,\rm in},\end{aligned} \tag{3}$$

where p and q are dimensionless canonical position and momentum, with $p = i(b^\dagger - b)/\sqrt{2}$ and $q = (b + b^\dagger)/\sqrt{2}$, respectively. $\Delta_R' = \Delta_R + \Delta_F$ and $g_b = \sqrt{2}g$, and $\kappa_L = \omega_L/Q_L$ ($\kappa_R = \omega_R/Q_R$) is the dissipation rate and Q_L (Q_R) is the quality factor of the left (right) cavity. $\gamma_m = \omega_m/Q_M$ is the damping rate with Q_M the quality factor of the mechanical mode. Moreover, ξ is the zero-mean Brownian stochastic operator, $\langle\xi(t)\rangle = 0$, resulting from the coupling of the mechanical resonator with the corresponding thermal environment and satisfying the correlation function [87]

$$\langle\xi(t)\xi(t')\rangle = \frac{1}{2\pi}\int d\omega e^{-i\omega(t-t')}\Gamma_m(\omega), \tag{4}$$

where

$$\Gamma_m(\omega) = \frac{\omega\gamma_m}{2\omega_m}\left[1 + \coth\left(\frac{\hbar\omega}{2k_B T}\right)\right], \tag{5}$$

T is effective temperature of the environment of the mechanical resonator, and k_B is the Boltzmann constant. The annihilation operators $a_{L,\rm in}$ and $a_{R,\rm in}$ are, respectively, the input vacuum noise operators of the optical cavity and the OM cavity with zero mean value, i.e., $\langle a_{L,\rm in}\rangle = \langle a_{R,\rm in}\rangle = 0$, and they comply with the time-domain correlation functions [88,89]

$$\begin{aligned}\langle a_{K,\rm in}^\dagger(t)a_{K,\rm in}(t')\rangle &= 0, \\ \langle a_{K,\rm in}(t)a_{K,\rm in}^\dagger(t')\rangle &= \delta(t - t'),\end{aligned} \tag{6}$$

for $K = L, R$. Because the whole system interacts with a low-temperature environment (here we consider 0.1 mK), we neglect the mean thermal photon numbers at optical frequencies in the two cavities. In order to linearize the dynamics around the steady state of the system, we expend the operators as the sum of its steady-state mean values and a small fluctuation with zero mean value around it; that is, $a_L = \alpha + \delta a_L$, $a_R = \beta + \delta a_R$, $q = q_s + \delta q$, and $p = p_s + \delta p$. By neglecting higher-order terms, $\delta a_L^\dagger \delta a_L$, the linearized equations of the fluctuation terms can be written as

$$\begin{aligned}\frac{d}{dt}\delta q &= \omega_m \delta p, \\ \frac{d}{dt}\delta p &= -\omega_m \delta q - g_b(\beta^*\delta a_R + \beta\delta a_R^\dagger) - \frac{\gamma_m}{2}\delta p + \xi, \\ \frac{d}{dt}\delta a_L &= -\left(\frac{\kappa_L}{2} + i\Delta_L\right)\delta a_L - iJ\delta a_R + \sqrt{\kappa_L}a_{L,\rm in}, \\ \frac{d}{dt}\delta a_R &= -\left(\frac{\kappa_R}{2} + i\Delta_R'\right)\delta a_R - iJ\delta a_L - ig_b q_s \delta a_R \\ &- ig_b\beta\delta q + \sqrt{\kappa_R}a_{R,\rm in}.\end{aligned} \tag{7}$$

These equations can be solved in the frequency domain (see Appendix B). In particular, we find

$$\begin{aligned}\delta a_L(\omega) &= E(\omega)a_{L,\rm in}(\omega) + F(\omega)a_{L,\rm in}^\dagger(\omega) + G(\omega)a_{R,\rm in}(\omega) \\ &+ H(\omega)a_{R,\rm in}^\dagger(\omega) + Q(\omega)\xi(\omega),\end{aligned} \tag{8}$$

where

$$\begin{aligned}E(\omega) &= \sqrt{\kappa_L}\frac{A_1(\omega)}{A_5(\omega)}, \\ F(\omega) &= -\sqrt{\kappa_L}\frac{A_2(\omega)}{A_5(\omega)}, \\ G(\omega) &= \sqrt{\kappa_R}\frac{A_3(\omega)}{A_5(\omega)}, \\ H(\omega) &= -\sqrt{\kappa_R}\frac{A_4(\omega)}{A_5(\omega)}, \\ Q(\omega) &= -i\frac{g_b\chi(\omega)}{\omega_m A_5(\omega)}[\beta A_3(\omega) + \beta^* A_4(\omega)],\end{aligned} \tag{9}$$

and

$$
\begin{aligned}
A_1(\omega) &= \left[\left(\frac{\kappa_R}{2}+i\omega\right)^2+\Delta_R''^2\right]V_1^-(\omega)\\
&\quad -g_b^4|\beta|^4\left[\frac{\chi(\omega)}{\omega_m}\right]^2 V_1^-(\omega)+J^2V_2^+,\\
A_2(\omega) &= -iJ^2g_b^2\beta^2\frac{\chi(\omega)}{\omega_m},\\
A_3(\omega) &= -iJV_1^-(\omega)V_2^- - iJ^3,\\
A_4(\omega) &= -Jg_b^2\beta^2\frac{\chi(\omega)}{\omega_m}V_1^-(\omega),\\
A_5(\omega) &= V_1^+A_1(\omega)+iJA_3(\omega),
\end{aligned}
\tag{10}
$$

where we introduced the auxiliary functions

$$
\begin{aligned}
\Delta_R'' &= \Delta_R' + g_b q_s - g_b^2|\beta|^2\chi(\omega),\\
\chi(\omega) &= \omega_m^2/\left(\omega_m^2-\omega^2+\frac{i\omega\gamma_m}{2}\right),\\
V_1^{\pm}(\omega) &= \frac{\kappa_L}{2}\pm i(\Delta_L-\omega),\\
V_2^{\pm}(\omega) &= \frac{\kappa_R}{2}\pm i(\Delta_R-\omega).
\end{aligned}
\tag{11}
$$

3. NONRECIPROCAL OPTICAL CORRELATIONS

Now, we focus on the statistical properties of photons in an optical cavity, which are described quantitatively via the normalized zero-time-delay second-order correlation function $g_L^{(2)}(0)=\langle a_L^{\dagger 2}a_L^2\rangle/\langle a_L^\dagger a_L\rangle^2$ [29,89]. By taking the semiclassical approximation, i.e., $a_L=\alpha+\delta a_L$, the correlation function $g_L^{(2)}(0)$ can be given as [29]

$$
g_L^{(2)}(0)=\frac{|\alpha|^4+4|\alpha|^2\mathcal{R}_1+2\,\mathrm{Re}[\alpha^{*2}\mathcal{R}_2]+\mathcal{R}_3}{(|\alpha|^2+\mathcal{R}_1)^2},
\tag{12}
$$

where $\mathcal{R}_1=\langle\delta a_L^\dagger(t)\delta a_L(t)\rangle$, $\mathcal{R}_2=\langle[\delta a_L(t)]^2\rangle$, and $\mathcal{R}_3=\langle\delta a_L^\dagger(t)\delta a_L^\dagger(t)\delta a_L(t)\delta a_L(t)\rangle=2\mathcal{R}_1+|\mathcal{R}_2|^2$.

From Eq. (8), the correlation between $\delta a_L(t)$ and $\delta a_L^\dagger(t)$ can be calculated as

$$
\langle\delta a_L^\pm(t)\delta a_L(t)\rangle=\frac{1}{2\pi}\int_{-\infty}^{+\infty}X_{a_L^\pm a_L}\mathrm{d}\omega,
\tag{13}
$$

where

$$
\begin{aligned}
&\delta a_L^+(t)=\delta a_L^\dagger(t),\delta a_L^-(t)=\delta a_L(t),\quad\text{and}\\
&X_{a_L^\dagger a_L}=|Q(-\omega)|^2\Gamma_m(-\omega)+|F(-\omega)|^2+|H(-\omega)|^2,\\
&X_{a_La_L}=Q(\omega)Q(-\omega)\Gamma_m(-\omega)+E(\omega)F(-\omega)\\
&\qquad+G(\omega)H(-\omega).
\end{aligned}
\tag{14}
$$

To obtain more accurate results, we introduce the density operator $\rho(t)$ and numerically calculate the normalized zero-time-delay second-order correlation by the Lindblad master equation [90]:

$$
\begin{aligned}
\dot\rho &= \frac{1}{i\hbar}[\mathcal{H},\rho]+\frac{\kappa_L}{2}\mathcal{L}[a_L](\rho)+\frac{\kappa_R}{2}\mathcal{L}[a_R](\rho)\\
&\quad+\frac{\gamma_m}{2}(\bar n_m+1)\mathcal{L}[b](\rho)+\frac{\gamma_m}{2}\bar n_m\mathcal{L}[b^\dagger](\rho),
\end{aligned}
\tag{15}
$$

where $\mathcal{L}[o](\rho)=2o\rho o^\dagger-o^\dagger o\rho-\rho o^\dagger o$ are the Lindblad superoperators [89], for $o=a_L$, a_R, b, and $b^\dagger$, and $\bar n_m=1/[\exp(\hbar\omega_m/k_BT)-1]$ is the mean thermal phonon number of the mechanical mode at temperature T.

The second-order correlation function $g_L(2)(0)$ is shown in Fig. 2 as a function of optical detuning Δ/κ and angular velocity Ω. We assume $\Delta_L=\Delta_R-\delta=\Delta$ and $\kappa_L=\kappa_R=\kappa$ and use experimentally feasible parameters [53,83,91–95], that is, $\lambda=1550$ nm, $Q_L=3\times10^7$, $r=0.3$ mm, $n=1.44$, $m=5\times10^{-11}$ kg, and $P_{\mathrm{in}}=2\times10^{-17}$ W. Q_L is typically 10^6–10^{12} [92,94,95], g is typically 10^3–10^6 Hz [83,91,92] in optical microresonators, and $g_L^{(2)}(0)\sim0.37$ [36,37] was achieved experimentally. J can be adjusted by changing the distance of the double resonators [72]. In a recent experiment, autocorrelation measurements ranging from $g^{(2)}(0)=6\times10^{-3}$ to 2 were achieved with an average fidelity of 0.998 in a photon-number-resolving detector [96]. Moreover, we set $\Omega=12$ kHz, which is experimentally feasible. The resonator with a radius of $r=1.1$ mm can spin at an angular velocity of $\Omega=6.6$ kHz [55]. Using a levitated OM system [97,98], Ω can be increased even up to GHz values.

Our analytical results agree well with the numerical one. In the case of a nonspinning resonator, as shown in Fig. 2(a), $g_L^{(2)}(0)$ is reciprocal regardless of the direction of the driving light, and always has a dip at $\Delta/\kappa\approx-0.29$ and a peak at $\Delta/\kappa\approx0.166$, corresponding to strong photon antibunching and photon bunching, respectively [29]. The physical origin of the strong photon antibunching is the destructive interference between the direct and indirect paths of two-photon excitations, i.e.,

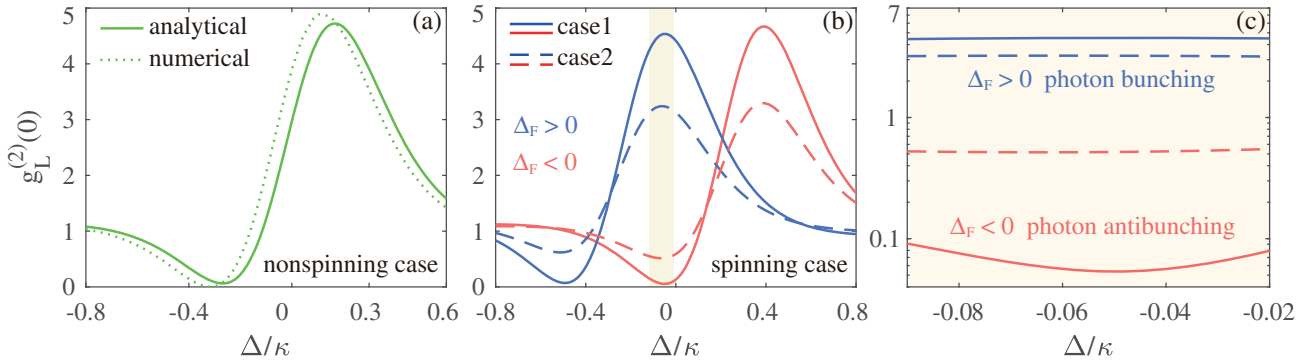

Fig. 2. Correlation function $g_L^{(2)}(0)$ versus optical detuning Δ/κ (in units of cavity loss rate $\kappa_L=\kappa_R=\kappa$) with (a) $\Omega=0$ and (b) $\Omega=12$ kHz, which is found numerically (solid curves) and analytically (dotted curve). The PB can be generated (red curves) or suppressed (blue curves) for different driving directions, which can be seen more clearly in panel (c). The other parameters are $g/\kappa=0.63$, $\omega_m/\kappa=10$ [91], $J/\kappa=3$, $T=0.1$ mK (case 1), and $g/\kappa=0.1$ [28], $\omega_m/\kappa=30$ [92], $J/\kappa=20$, $T=1$ mK (case 2).

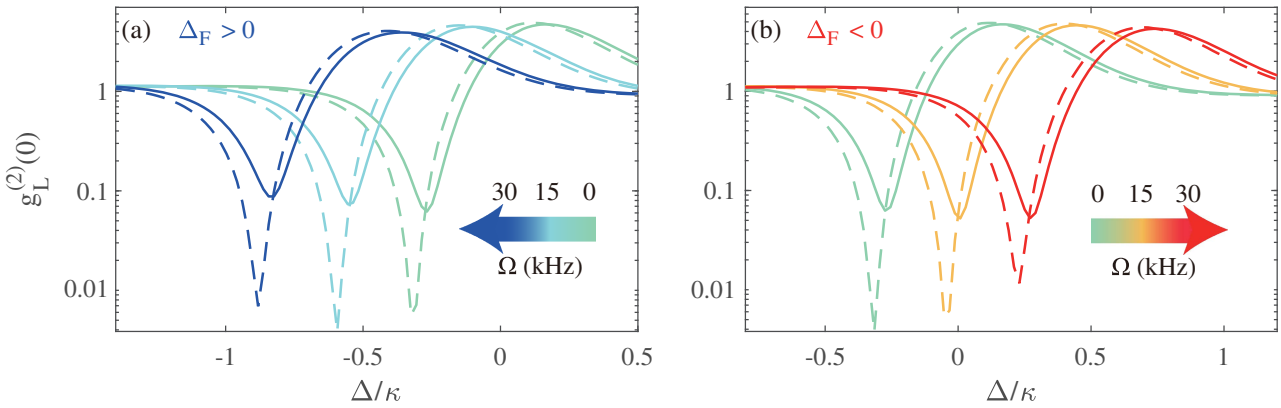

Fig. 3. Correlation function $g_L^{(2)}(0)$ versus optical detuning Δ/κ (in units of cavity loss rate $\kappa_L = \kappa_R = \kappa$) at various angular velocities Ω upon driving the device from (a) the right-hand side or (b) the left-hand side. The dashed curves show our approximate analytical results, given in Eq. (12), whereas the solid curves are our numerical solutions. The other parameters are the same as those in Fig. 2 (case 1).

$$|1,0\rangle \xrightarrow{\sqrt{2}\epsilon_d} |2,0\rangle, |1,0\rangle \xrightarrow{J} |0,1\rangle \xrightarrow{\epsilon_d} |1,1\rangle \xrightarrow{\sqrt{2}J} |2,0\rangle.$$

In contrast, for a spinning device, $g_L^{(2)}(0)$ exhibits giant nonreciprocity, which can be seen in Fig. 2(b). The PB can be generated, i.e., $g_L^{(2)}(0) \sim 0.06$, for $\Delta_F < 0$, whereas it is significantly suppressed, i.e., $g_L^{(2)}(0) \sim 4.72$, for $\Delta_F > 0$; this can be seen more clearly in Fig. 2(c). Nonreciprocal UPB induced by the Fizeau light-dragging effect, with difference in $g_L^{(2)}(0)$ up to two orders of magnitude for opposite directions, can be achieved even with weak nonlinearity and, to our knowledge, has not been studied previously. Furthermore, in Fig. 2(b), we use two sets of parameters for solid (case 1) and dashed curves (case 2), respectively. It can be seen that nonreciprocity still exists in a parameter range closer to that in the experiment.

Since the anharmonicity of the system is very small, destructive quantum interference (rather than anharmonicity) is responsible for observing strong photon antibunching (referred to as UPB) and photon bunching (referred to as photon-induced tunneling) in the spinning devices, as shown in Fig. 1 and confirmed by our analytical calculations. Note that the role of complete (incomplete) destructive quantum interference is the same in both spinning and non-spinning UPB systems, and, thus, we refer to Ref. [24] where this interference-based mechanism was first explained in detail. Spinning the OM resonator results in different Fizeau drag Δ_F for the counter-circulating whispering-gallery modes of the resonator. By driving the system from the left-hand side, direct excitation from state $|1,0\rangle$ to state $|2,0\rangle$ will be forbidden by destructive quantum interference with the indirect paths of two-photon excitations, leading to photon antibunching. In contrast, photon bunching occurs when the system is driven from the right side, due to lack of complete destructive quantum interference between the indicated levels [99]. Increasing the angular velocity results in an opposing frequency shift of $\eta\Omega$ for light coming from opposite directions. $g_L^{(2)}(0)$ also shifts linearly with Ω, but with different directions for $\Delta_F < 0$ and $\Delta_F > 0$; that is, we observe either a blue shift [see Fig. 3(a)] or a red shift [see Fig. 3(b)] with $\Delta_F > 0$ or $\Delta_F < 0$, respectively. A highly tunable nonreciprocal UPB device is thus achievable, by flexible tuning of Ω and Δ/κ. In addition, since $g_L^{(2)}(0)$ is sensitive to Ω, this may also indicate a way for accurate measurements of velocity.

4. OPTIMAL PARAMETERS FOR STRONG ANTIBUNCHING

As discussed above, UPB can be generated nonreciprocally. In this section, we analytically derive the optimal conditions for

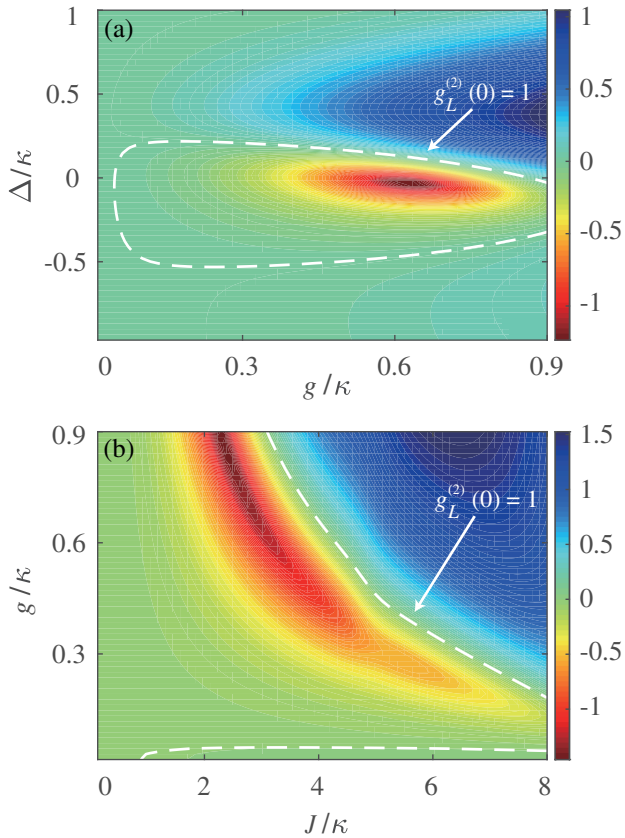

Fig. 4. Correlation function $g_L^{(2)}(0)$ in logarithmic scale [i.e., $\log_{10} g_L^{(2)}(0)$] versus (a) radiation-pressure coupling g/κ (in units of cavity loss rate $\kappa = \kappa_L = \kappa_R$) and optical detuning Δ/κ, and (b) coupling strength of the resonators J/κ and radiation-pressure coupling g/κ for optical detuning of $\Delta/\kappa = -0.05$. The angular velocity is $\Omega = 12$ kHz and the white dashed curve corresponds to $g_L^{(2)}(0) = 1$. The other parameters are the same as those in Fig. 3.

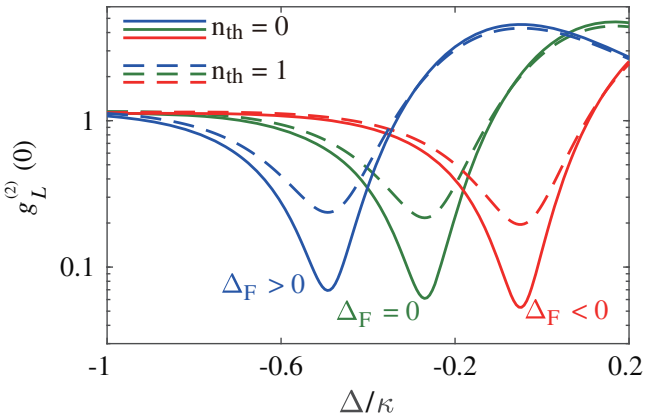

Fig. 5. Correlation function $g_L^{(2)}(0)$ versus optical detuning Δ/κ (in units of cavity loss rate $\kappa_L = \kappa_R = \kappa$) with varied mean thermal phonon numbers nth for various angular velocities Ω, and the resulting Fizeau shifts Δ_F. The other parameters are the same as those in Fig. 4.

strong antibunching. Here we apply the method described in Ref. [24], which is based on the evolution of a complex non-Hermitian Hamiltonian, as given in Appendix C. Thus, our solution corresponds to only a semi-classical approximation of the solution of the quantum master equation, given in Eq. (15), where the terms corresponding to quantum jumps are ignored.

Since the phonon states can be decoupled from the photon states by using the unitary operator $U = \exp[-g(b^\dagger - b)/\omega_m]$, the states of the system can be expressed as $|\psi\rangle = |\varphi\rangle|\phi_m\rangle$, where $|\varphi\rangle$ and $|\phi_m\rangle$ are the photon states and phonon states, respectively. Under the weak-driving condition, we make the ansatz [24]

$$|\varphi\rangle = C_{00}|0,0\rangle + C_{10}|1,0\rangle + C_{01}|0,1\rangle + C_{20}|2,0\rangle + C_{11}|1,1\rangle + C_{02}|0,2\rangle, \tag{16}$$

and consider that $C_{mn} \ll C_{m'n'} \ll C_{00}$ for $m+n=2$, $m'+n'=1$, and the condition of $C_{20}=0$; the optimal conditions are given by fixing J and κ (see Appendix C):

$$\Delta_{opt} \approx \frac{-a_3 + \mathrm{sgn}(E)\sqrt{\lambda_1} - \sqrt{\lambda_2}}{4a_4},$$
$$g_{opt} = \sqrt{-\frac{\omega_m[\Delta_{opt}(4\Delta_{opt}^2 + 5\kappa^2) + \Delta_F\lambda_3]}{2(2J^2 - \kappa^2) + 2\Delta_F\lambda_4}}, \tag{17}$$

the signal function $\mathrm{sgn}(E)$, $a_3 = -96\Delta_F\kappa$, and $\lambda_{1,2}$, which are defined in Appendix C, are related to the Fizeau drag Δ_F.

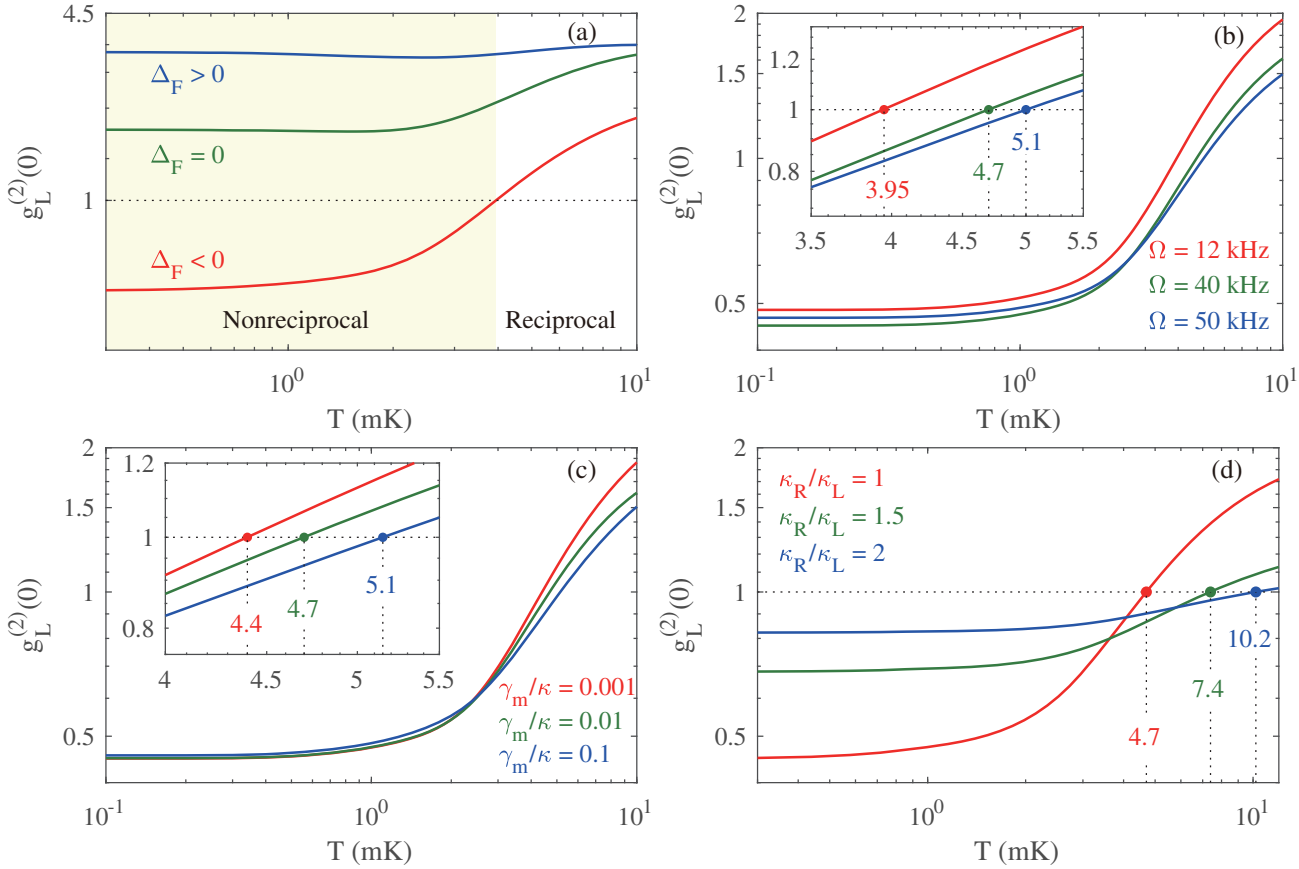

Fig. 6. (a) Correlation function $g_L^{(2)}(0)$ versus effective temperature T of the environment of the mechanical resonator for three values of Fizeau shift Δ_F ($\Delta_F > 0$, $\Delta_F = 0$, and $\Delta_F < 0$) for optimal values of Δ_{opt} and g_{opt}. The other parameters are set the same as in case 2 in Fig. 2. Also shown is the correlation function $g_L^{(2)}(0)$ versus T for various values of (b) spinning frequency, (c) mechanical decay, and (d) cavity decay, assuming the device is driven from the left-hand side and optical detuning is fixed at the optimal values.

Physically, this means that the position of the minimum of $g_L^{(2)}(0)$ is determined by the detuning between the two cavity fields. Thus, Δ_F can lead to a shift of the minimum of $g_L^{(2)}(0)$ to achieve nonreciprocity.

In order to visualize UPB more clearly, we show the contour plots of $g_L^{(2)}(0)$ in logarithmic scale [i.e., $\log_{10} g_L^{(2)}(0)$] as a function of g/κ and Δ/κ in Fig. 4(a). By fixing $\Delta/\kappa = -0.05$, we obtain the function of $g_L^{(2)}(0)$ in logarithmic scale versus the coupling strengths J/κ and g/κ of the resonators, as shown in Fig. 4(b). These plots show that strong photon antibunching occurs exactly at the values predicted by our analytical calculations in Eq. (17). Moreover, by computing $g_L^{(2)}(0)$ as a function of Δ/κ and Ω with different mean thermal phonon numbers nth, as shown in Fig. 5, we confirm that rotation-induced nonreciprocity can still exist by considering thermal phonon noises. We note that thermal phonons greatly affect the correlation $g_L^{(2)}(0)$ of photons and tend to destroy PB. Thus, to show this effect, in Fig. 6(a) we plot the correlation $g_L^{(2)}(0)$ as a function of temperature T for various Fizeau shifts. We see that nonreciprocal UPB can be observed below the critical temperature $T_0 \approx 4$ mK (5 mK) for the spinning frequency of $\Omega = 12$ kHz ($\Omega = 50$ kHz) [see Fig. 6(b)]. By further increasing the optical dissipation of the OM cavity, as shown in Fig. 6(d), the critical temperature T_0 can be made to reach a value of 10 mK.

Finally, we note that a state (generated via UPB or another effect) with vanishing (or almost vanishing) second-order photon-number correlations, $g^{(2)}(0) \approx 0$, is not necessarily a good single-photon source, i.e., the state might not be a (partially incoherent) superposition of only the vacuum and single-photon states. A good single-photon source is characterized not only by $g^{(2)}(0) \approx 0$, but also by vanishing higher-order photon-number correlation functions, $g^{(n)}(0) \approx 0$ for $n > 2$. In UPB, $g^{(n)}(0)$ for $n > 2$ can be greater than $g^{(2)}(0) \approx 0$, or even greater than 1 [100]. Indeed, a standard analytical method for analyzing UPB, as proposed by Bamba *et al.* [24] and applied here, is based on expanding the wave function $|\varphi\rangle$ of a two-resonator system in the power series $|\varphi\rangle = \sum C_{n,m}|n,m\rangle$ up to the terms $C_{n,2-n}$ $(n = 0, 1, 2)$ only, as given in Eq. (16). To obtain the optimal system parameters, which minimize $g^{(2)}(0)$ in UPB, this method requires setting $C_{2,0} = 0$ as set in Appendix C. Actually, the same expansion of $|\varphi\rangle$ and the same ansatz are made in Ref. [24]. These assumptions imply that higher-order correlation functions $g^{(n)}(0)$ with $n = 3, 4, \ldots$ vanish too. However, the truncation of the above expansion at the terms $C_{n,2-n}$ is often not justified for a system exhibiting UPB. Indeed, we find parameters for our system for which $g^{(2)}(0) \approx 0$ and, simultaneously, $g^{(3)}(0) > 1$. We have confirmed this by precise numerical calculation of the steady states of our system based on the non-Hermitian Hamiltonian, given in Eq. (C1), in a Hilbert space larger than 4×4.

5. CONCLUSIONS

In summary, we studied nonreciprocal UPB in a system consisting of a purely optical resonator and a spinning OM resonator. Due to interference between two-photon excitation paths and the Sagnac effect, UPB can be generated nonreciprocally in our system; that is, UPB can occur when the system is driven from one direction but not from the other, even under weak OM interactions. The optimal conditions for one-way UPB were presented analytically. Moreover, we found that this quantum nonreciprocity can still exist by considering thermal phonon noises.

Concerning a possible experimental implementation of nonreciprocal UPB, it is worth noting that UPB for non-spinning devices has already been demonstrated experimentally in two recent works [36,37]. A number of experiments (including a very recent work [55]) have shown nonreciprocal quantum effects in spinning devices. So the main experimental task for achieving nonreciprocal UPB in a spinning device would be to combine the experimental setups of, e.g., Refs. [36,37,55] into a single spinning UPB setup.

Our proposal provides a feasible method to control the behavior of one-way photons, with potential applications in achieving, e.g., photonic diodes or circulators, quantum chiral communications, and nonreciprocal light engineering in the deep quantum regime.

APPENDIX A: DERIVATION OF EFFECTIVE HAMILTONIAN

The coupled system can be described by the Hamiltonian

$$\begin{aligned} H &= H_0 + H_{\rm in} + H_{\rm dr}, \\ H_0 &= \hbar\omega_L a_L^\dagger a_L + \hbar(\omega_R + \Delta_F) a_R^\dagger a_R + \hbar\omega_m b^\dagger b, \\ H_{\rm in} &= \hbar J(a_L^\dagger a_R + a_R^\dagger a_L) + \hbar g a_R^\dagger a_R (b^\dagger + b), \\ H_{\rm dr} &= i\hbar\epsilon_d (a_L^\dagger e^{-i\omega_d t} - a_L e^{i\omega_d t}), \end{aligned} \tag{A1}$$

where a_L ($a_L^\dagger$) and a_R ($a_R^\dagger$) are the photon annihilation (creation) operators for the cavity modes of the optical cavity (denoted with the subscript L) and the OM cavity (denoted with the subscript R), respectively. b ($b^\dagger$) is the annihilation (creation) operator for the mechanical mode of the OM cavity. The frequencies of the cavity fields are denoted with ω_L and ω_R. J is the coupling strength between the two resonators, and $g = \omega_R / r[\hbar/(2m\omega_m)]^{1/2}$ is the OM coupling strength between the optical mode and the mechanical mode in the OM cavity. $\epsilon_d = \sqrt{\kappa_L P_{\rm in}/(\hbar\omega_d)}$ denotes the driving strength that is coupled into the compound system through the optical fiber waveguide.

Using the unitary operator $U = \exp[-g(b^\dagger - b)/\omega_m]$ for the Hamiltonian (A1), we obtain a Kerr-type Hamiltonian [82]

$$\begin{aligned} H_{\rm eff} &= U^\dagger H U \\ &= \hbar\omega_L a_L^\dagger a_L + \hbar(\omega_R + \Delta_F) a_R^\dagger a_R - \hbar\delta (a_R^\dagger a_R)^2 \\ &\quad + \hbar J[a_L^\dagger a_R e^{-\delta(b^\dagger - b)} + a_L a_R^\dagger e^{\delta(b^\dagger - b)}] \\ &\quad + i\hbar\epsilon_d (a_L^\dagger e^{-i\omega_d t} - a_L e^{i\omega_d t}), \end{aligned} \tag{A2}$$

where $\delta = g^2/\omega_m$. Under the conditions $g/\omega_m \ll 1$ and $J < \omega_m/2$, the Hamiltonian (A2) can be read as

$$H'_{\rm eff} = \hbar\omega_L a_L^\dagger a_L + \hbar(\omega_R + \Delta_{\rm F}) a_R^\dagger a_R - \hbar\delta(a_R^\dagger a_R)^2 + \hbar J(a_L^\dagger a_R + a_L a_R^\dagger) + i\hbar\epsilon_d(a_L^\dagger e^{-i\omega_d t} - a_L e^{i\omega_d t}). \tag{A3}$$

APPENDIX B: FOURIER ANALYSIS OF FLUCTUATION TERMS

According to the Heisenberg equations of motion of Hamiltonian (2), and using the semi-classical approximation method, i.e., $a_L = \alpha + \delta a_L$, $a_R = \beta + \delta a_R$, $q = q_s + \delta q$, and $p = p_s + \delta p$, the steady-state values of the system satisfy the equations

$$\begin{aligned} 0 &= \left(\frac{\kappa_L}{2} + i\Delta_L\right)\alpha + iJ\beta - \epsilon_d, \\ 0 &= \left[\frac{\kappa_R}{2} + i(\Delta'_R + g_b q_s)\right]\beta - iJ\alpha, \\ 0 &= \omega_m q_s - g_b|\beta|^2. \end{aligned} \tag{B1}$$

Then we obtain

$$b_3 q_s^3 + b_2 q_s^2 + b_1 q_s + b_0 = 0, \tag{B2}$$

where

$$\begin{aligned} b_0 &= g_b J^2 \epsilon_d^2, \\ b_1 &= \omega_m\left(\frac{\kappa_L\kappa_R}{4} + J^2\right)^2 + \omega_m\left(\frac{\kappa_L\Delta'_R}{2} + \frac{\kappa_R\Delta_L}{2}\right)^2 - \omega_m\Delta_L\Delta'_R\left(\frac{\kappa_L\kappa_R}{2} + 2J^2 - \Delta_L\Delta'_R\right), \\ b_2 &= 2\omega_m g_b\left[\frac{\kappa_L^2\Delta'_R}{4} + \Delta_L(\Delta_L\Delta'_R - J^2)\right], \\ b_3 &= \omega_m g_b^2\left(\frac{\kappa_L^2}{4} + \Delta_L^2\right). \end{aligned} \tag{B3}$$

The fluctuation terms of the system can be written as

$$\begin{aligned} \frac{\mathrm{d}}{\mathrm{d}t}\delta q &= \omega_m\delta p, \\ \frac{\mathrm{d}}{\mathrm{d}t}\delta p &= -\omega_m\delta q - g_b(\beta^*\delta a_R + \beta\delta a_R^\dagger) - \frac{\gamma_m}{2}\delta p + \xi, \\ \frac{\mathrm{d}}{\mathrm{d}t}\delta a_L &= -\left(\frac{\kappa_L}{2} + i\Delta_L\right)\delta a_L - iJ\delta a_R + \sqrt{\kappa_L}a_{L,\rm in}, \\ \frac{\mathrm{d}}{\mathrm{d}t}\delta a_R &= -\left(\frac{\kappa_R}{2} + i\Delta'_R\right)\delta a_R - iJ\delta a_L - ig_b q_s\delta a_R - ig_b\beta\delta q + \sqrt{\kappa_R}a_{R,\rm in}, \end{aligned} \tag{B4}$$

where we have neglected higher-order terms, $\delta a_L^\dagger\delta a_L$. Here, the steady-state mean value q_s is numerically solved from Eqs. (B2) and (B3).

By introducing the Fourier transform to the fluctuation equations, we find

$$\begin{aligned} i\omega\delta a_L(\omega) &= -\left(\frac{\kappa_L}{2} + i\Delta_L\right)\delta a_L(\omega) - iJ\delta a_R(\omega) + \sqrt{\kappa_L}a_{L,\rm in}(\omega), \\ i\omega\delta a_R(\omega) &= -\left(\frac{\kappa_R}{2} + i\Delta'''_R\right)\delta a_L(\omega) - iJ\delta a_R(\omega) - ig_b\beta\delta q(\omega) + \sqrt{\kappa_R}a_{R,\rm in}(\omega), \\ i\omega\delta q(\omega) &= \omega_m\delta p(\omega), \\ i\omega\delta p(\omega) &= -\omega_m\delta q(\omega) - g_b[\beta^*\delta a_R(\omega) + \beta\delta a_R^\dagger(\omega)] - \frac{\gamma_m}{2}\delta p(\omega) + \xi(\omega), \end{aligned} \tag{B5}$$

where $\Delta'''_R = \Delta'_R + g_b q_s$; then we obtain

$$\delta q(\omega) = -g_b\beta^*\chi(\omega)\delta a_R(\omega) - g_b\beta\chi(\omega)\delta a_R^\dagger(\omega) + \chi(\omega)\xi(\omega), \tag{B6}$$

where

$$\chi(\omega) = \frac{\omega_m}{\omega_m^2 - \omega^2 + i\omega\gamma_m/2}. \tag{B7}$$

Substituting Eq. (B6) into Eq. (B5), we have

$$M(\omega)\delta a_R(\omega) = ig_b^2\beta^2\chi(\omega)\delta a_R^\dagger(\omega) - ig_b\beta\chi(\omega)\xi(\omega) - iJ\delta_L(\omega) + \sqrt{\kappa_R}a_{R,\rm in}(\omega), \tag{B8}$$

where

$$M(\omega) = \frac{\kappa_R}{2} + i\omega + i\Delta'''_R - i|\beta|^2 g_b^2\chi(\omega). \tag{B9}$$

According to Eq. (B5), we obtain

$$\begin{aligned} i\omega\delta a_L^\dagger(\omega) &= -\left(\frac{\kappa_L}{2} - i\Delta_L\right)\delta a_L^\dagger(\omega) + iJ\delta a_R^\dagger(\omega) + \sqrt{\kappa_L}a_{L,\rm in}^\dagger(\omega), \\ i\omega\delta a_R^\dagger(\omega) &= -\left(\frac{\kappa_R}{2} - i\Delta'''_R\right)\delta a_R^\dagger(\omega) + iJ\delta a_R^\dagger(\omega) + ig_b\beta\delta q^\dagger(\omega) + \sqrt{\kappa_R}a_{R,\rm in}^\dagger(\omega), \\ i\omega\delta q^\dagger(\omega) &= \omega_m\delta p^\dagger(\omega), \\ i\omega\delta p^\dagger(\omega) &= -\omega_m\delta q^\dagger(\omega) - g_b[\beta\delta a_R^\dagger(\omega) + \beta^*\delta a_R(\omega)] - \frac{\gamma_m}{2}\delta p^\dagger + \xi^\dagger(\omega), \end{aligned} \tag{B10}$$

then we have

$$N(\omega)\delta a_R(\omega) = -ig_b^2\beta^{*2}\chi(\omega)\delta a_R^\dagger(\omega) + ig_b\beta^*\chi(\omega)\xi^\dagger(\omega) + iJ\delta a_L^\dagger(\omega) + \sqrt{\kappa_R}a_{R,\rm in}^\dagger(\omega), \tag{B11}$$

where

$$N(\omega) = \frac{\kappa_R}{2} + i\omega - i\Delta'''_R + i|\beta|^2 g_b^2\chi(\omega). \tag{B12}$$

From Eq. (B10), we have

$$V(\omega)\delta a_L^\dagger(\omega) = iJ\delta a_R^\dagger(\omega) + \sqrt{\kappa_L}a_{L,\rm in}^\dagger(\omega), \tag{B13}$$

where $V(\omega) = \kappa_L/2 + i\omega - i\Delta_L$. Substituting Eq. (B13) into Eq. (B11), we find

$$T(\omega)\delta a_R^\dagger(\omega) = -i\chi(\omega)g_b^2\beta^{*2}V(\omega)\delta a_R(\omega) + i\chi(\omega)g_b\beta^* V(\omega)\xi^\dagger(\omega) + iJ\sqrt{\kappa_L}a_{L,\mathrm{in}}^\dagger(\omega) + \sqrt{\kappa_R}V(\omega)a_{R,\mathrm{in}}^\dagger(\omega), \quad \textbf{(B14)}$$

where $T(\omega) = N(\omega)V(\omega) + J^2$. Substituting Eq. (B14) into Eq. (B8), we obtain

$$F_R(\omega)\delta a_R(\omega) = -\chi^2(\omega)g_b^3\beta|\beta|^2\ V(\omega)\xi^\dagger(\omega) - ig_b\beta\chi(\omega)T(\omega)\xi(\omega) - Jg_b^2\beta^2\chi(\omega)\sqrt{\kappa_L}a_{L,\mathrm{in}}^\dagger + ig_b^2\beta^2\chi(\omega)\sqrt{\kappa_R}V(\omega)a_{R,\mathrm{in}}^\dagger(\omega) - iJT(\omega)a_{L,\mathrm{in}} - \sqrt{\kappa_R}T(\omega)a_{R,\mathrm{in}}, \quad \textbf{(B15)}$$

where the auxiliary function is $F_R(\omega) = M(\omega)T(\omega) - \chi^2(\omega)V(\omega)g_b^4|\beta|^4$. Substituting Eq. (B15) into Eq. (B5), we have

$$F_L(\omega)\delta a_L(\omega) = iJ\chi^2(\omega)g_b^3\beta|\beta|^2\ V(\omega)\xi^\dagger(\omega) - g_b\beta\chi(\omega)JT(\omega)\xi(\omega) + iJ^2g_b^2\beta^2\chi(\omega)\sqrt{\kappa_L}a_{L,\mathrm{in}}^\dagger + Jg_b^2\beta^2\chi(\omega)\sqrt{\kappa_R}V(\omega)a_{R,\mathrm{in}}^\dagger(\omega) - iJ\sqrt{\kappa_R}T(\omega)a_{R,\mathrm{in}} - \sqrt{\kappa_L}[M(\omega)T(\omega) - U(\omega)]a_{L,\mathrm{in}}, \quad \textbf{(B16)}$$

where

$$F_L(\omega) = [M(\omega)T(\omega) - U(\omega)]V_1(\omega) + J^2T(\omega),$$
$$U(\omega) = -\chi^2(\omega)g_b^4|\beta|^4\left(i\omega + \frac{\kappa_L}{2} - i\Delta_L\right),$$
$$V_1(\omega) = \frac{\kappa_L}{2} + i\omega + i\Delta_L. \quad \textbf{(B17)}$$

Then we find

$$\delta a_L(\omega) = E(\omega)a_{L,\mathrm{in}}(\omega) + F(\omega)a_{L,\mathrm{in}}^\dagger(\omega) + G(\omega)a_{R,\mathrm{in}}(\omega) + H(\omega)a_{R,\mathrm{in}}^\dagger(\omega) + Q(\omega)\xi(\omega). \quad \textbf{(B18)}$$

According to similar calculations, we find

$$\delta a_L^\dagger(\omega) = E^*(-\omega)a_{L,\mathrm{in}}^\dagger(\omega) + F^*(-\omega)a_{L,\mathrm{in}}(\omega) + G^*(-\omega)a_{R,\mathrm{in}}^\dagger(\omega) + H^*(-\omega)a_{R,\mathrm{in}}(\omega) + Q^*(-\omega)\xi(\omega). \quad \textbf{(B19)}$$

Using the Fourier transform, we obtain

$$\langle a_{L,\mathrm{in}}(\omega)a_{L,\mathrm{in}}^\dagger(\omega')\rangle = \frac{1}{\sqrt{2\pi}}\int_{-\infty}^{\infty}\langle a_{L,\mathrm{in}}(t)e^{-i\omega t}\mathrm{d}t \times \frac{1}{\sqrt{2\pi}}\int_{-\infty}^{\infty}a_{L,\mathrm{in}}^\dagger(t')\rangle e^{-i\omega' t'}\mathrm{d}t' = \delta(\omega+\omega'), \quad \textbf{(B20)}$$

and

$$\langle a_{R,\mathrm{in}}(\omega)a_{R,\mathrm{in}}^\dagger(\omega')\rangle = \delta(\omega+\omega'). \quad \textbf{(B21)}$$

APPENDIX C: DERIVATION OF OPTIMAL PARAMETERS

According to the quantum-trajectory method [101], the non-Hermitian Hamiltonian of the system containing the optical decay and mechanical damping terms is given by [101]

$$H' = \hbar\left(\Delta_L - i\frac{\kappa_L}{2}\right)a_L^\dagger a_L + \hbar\left(\Delta_R' - i\frac{\kappa_R}{2}\right)a_R^\dagger a_R + \hbar\left(\omega_m - i\frac{\gamma_m}{2}\right)b^\dagger b + \hbar J(a_L^\dagger a_R + a_R^\dagger a_L) - \hbar\delta(a_R^\dagger a_R)^2 + i\hbar\epsilon_d(a_L^\dagger - a_L), \quad \textbf{(C1)}$$

where $\Delta_R' = \Delta_R + \Delta_F$.

Under the weak-driving conditions, we can make the ansatz [24]

$$|\varphi\rangle = C_{00}|0,0\rangle + C_{10}|1,0\rangle + C_{01}|0,1\rangle + C_{20}|2,0\rangle + C_{11}|1,1\rangle + C_{02}|0,2\rangle. \quad \textbf{(C2)}$$

Then we substitute the Hamiltonian [Eq. (C1)] and the general state [Eq. (C2)] into the Schrödinger equation

$$i\hbar\frac{\mathrm{d}|\varphi\rangle}{\mathrm{d}t} = H'|\varphi\rangle, \quad \textbf{(C3)}$$

and then we have

$$\begin{aligned}
H'C_{00}|0,0\rangle &= i\hbar\epsilon_d C_{00}|1,0\rangle,\\
H'C_{10}|1,0\rangle &= \hbar\delta_L C_{10}|1,0\rangle + \hbar J C_{10}|0,1\rangle + i\hbar\epsilon_d C_{10}\left(\sqrt{2}|2,0\rangle - |0,0\rangle\right),\\
H'C_{01}|0,1\rangle &= \hbar\delta_R C_{01}|0,1\rangle + \hbar J C_{01}|1,0\rangle + i\hbar\epsilon_d C_{01}|1,1\rangle,\\
H'C_{20}|2,0\rangle &= 2\hbar\delta_L C_{20}|2,0\rangle + \sqrt{2}\hbar J C_{20}|1,1\rangle + i\hbar\epsilon_d C_{20}\left(\sqrt{3}|3,0\rangle - \sqrt{2}|1,0\rangle\right),\\
H'C_{11}|1,1\rangle &= \hbar\delta_L C_{11}|1,1\rangle + \hbar\delta_R C_{11}|1,1\rangle + \sqrt{2}\hbar J C_{11}(|2,0\rangle + |0,2\rangle) + i\hbar\epsilon_d C_{11}\left(\sqrt{2}|2,1\rangle - |0,1\rangle\right),\\
H'C_{02}|0,2\rangle &= 2\hbar\delta_R C_{02}|0,2\rangle - 2\delta C_{02}|0,2\rangle + \sqrt{2}\hbar J C_{02}(|1,1\rangle + i\hbar\epsilon_d C_{02}|1,2\rangle, \quad \textbf{(C4)}
\end{aligned}$$

where the auxiliary functions are $\delta_L = \Delta_L - i\kappa_L/2$ and $\delta_R = \Delta_R' - i\kappa_R/2$, and we have ignored the effects of the mechanical model because the phonon states are decoupled from the photon states [see Eq. (C1)]. By comparing the coefficients, we have

$$\begin{aligned}
\frac{\partial C_{00}}{\partial t} &= \epsilon_d C_{10},\\
i\frac{\partial C_{10}}{\partial t} &= \delta_L C_{10} + JC_{01} - \sqrt{2}i\epsilon_d C_{20},\\
i\frac{\partial C_{01}}{\partial t} &= (\delta_R - \delta)C_{01} + JC_{10} - i\epsilon_d C_{11},\\
i\frac{\partial C_{11}}{\partial t} &= \delta_L C_{11} + (\delta_R - \delta)C_{11}\\
&\quad + \sqrt{2}J(C_{02} + C_{20}) + i\epsilon_d C_{01},\\
i\frac{\partial C_{02}}{\partial t} &= 2(\delta_R - \delta)C_{02} + \sqrt{2}JC_{11} - 2\delta C_{02},\\
i\frac{\partial C_{20}}{\partial t} &= 2(\delta_R - \delta)C_{20} + \sqrt{2}JC_{11} + \sqrt{2}i\epsilon_d C_{10}.
\end{aligned} \tag{C5}$$

Then the steady-state coefficients of the one- and two-particle states are given as

$$\begin{aligned}
0 &= \delta_L C_{10} + JC_{01} + i\epsilon_d C_{00},\\
0 &= \delta_R C_{01} + JC_{10},
\end{aligned} \tag{C6}$$

and

$$\begin{aligned}
0 &= 2\delta_L C_{20} + \sqrt{2}JC_{11} + i\sqrt{2}\epsilon_d C_{10},\\
0 &= (\delta_L + \delta_R)C_{11} + \sqrt{2}JC_{20} + \sqrt{2}JC_{02} + i\epsilon_d C_{01},\\
0 &= 2(\delta_R - \delta)C_{02} + \sqrt{2}JC_{11},
\end{aligned} \tag{C7}$$

where we have introduced the dissipative terms (proportional to κ_L and κ_R) and neglected the higher-order terms, as justified under the weak-driving conditions.

When we consider $\Delta_L = \Delta_R - \delta = \Delta$, $\delta = g^2/\omega_m$, $\kappa_L = \kappa_R = \kappa$, and the condition of $C_{20} = 0$, we have

$$\begin{aligned}
0 &= \kappa^2(2\delta - 6\Delta - 5\Delta_F^2) + 4\Delta^2(2\Delta - 2\delta - 5\delta\Delta_F^2)\\
&\quad + 4\Delta_F(4\Delta\Delta_F - 3\delta\Delta - \delta\Delta_F + \Delta_F^2) - 4J^2\delta,\\
0 &= 8\delta\Delta - 12\Delta^2 + \kappa^2 + \Delta_F(6\delta - 20\Delta - 8\Delta_F).
\end{aligned} \tag{C8}$$

By eliminating δ, we obtain

$$a_4\Delta^4 + a_3\Delta^3 + a_2\Delta^2 + a_1\Delta + a_0 = 0, \tag{C9}$$

where

$$\begin{aligned}
a_0 &= \kappa(4J^2 - 10\Delta_F^2)(\kappa^2 - 8\Delta_F^2) - 2\kappa(\kappa^4 - 44\Delta_F^4),\\
a_1 &= -8\Delta_F(6\Delta_F^2\kappa + 10J^2\kappa + 3),\\
a_2 &= -8\kappa(2\kappa^2 + 6J^2 + 13\Delta_F^2),\\
a_3 &= -96\Delta_F\kappa,\\
a_4 &= -32\kappa,
\end{aligned} \tag{C10}$$

then we find the optimal conditions

$$\begin{aligned}
\Delta_{opt} &\approx \frac{-a_3 + \mathrm{sgn}(E)\sqrt{\lambda_1} - \sqrt{\lambda_2}}{4a_4},\\
g_{opt} &= \sqrt{-\frac{\omega_m[\Delta_{opt}(4\Delta_{opt}^2 + 5\kappa^2) + \Delta_F\lambda_3]}{2(2J^2 - \kappa^2) + 2\Delta_F\lambda_4}},
\end{aligned} \tag{C11}$$

where

$$\begin{aligned}
\lambda_1 &= \frac{D + \sqrt[3]{z_1} + \sqrt[3]{z_2}}{3},\\
\lambda_2 &= \frac{2D - \sqrt[3]{z_1} - \sqrt[3]{z_2} + \sqrt[3]{z_3}}{3},\\
\lambda_3 &= 20\Delta_{opt}^2 - 8\Delta_{opt}\Delta_F - 4\Delta_F^2 + 5\kappa^2,\\
\lambda_4 &= 10\Delta_{opt}^2 + 3\Delta_{opt} + 2\Delta_F,
\end{aligned} \tag{C12}$$

and

$$\begin{aligned}
\mathrm{sgn}(E) &= \begin{cases} 1 & (E > 0),\\ -1 & (E < 0),\end{cases}\\
z_{1,2} &= AD + 3\frac{-B \pm \sqrt{B^2 - 4AC}}{2},\\
z_3 &= D^2 - D\left(\sqrt[3]{z_1} + \sqrt[3]{z_2}\right) + \left(\sqrt[3]{z_1} + \sqrt[3]{z_2}\right)^2 - 3A,\\
A &= D^2 - 3F,\\
B &= DF - 9E^2,\\
C &= F^2 - 3DE^2,\\
D &= 3a_3^2 - 8a_4a_2,\\
E &= -a_3^3 + 4a_4a_3a_2 - 8a_4^2a_1,\\
F &= 3a_3^4 + 16a_4^2a_2^2 - 16a_4a_3^2a_2 + 16a_4^2a_3a_1\\
&\quad - 64a_4^3a_0.
\end{aligned} \tag{C13}$$

Funding. National Natural Science Foundation of China (NSFC) (11474087, 11774086).

REFERENCES

1. L. Tian and H. J. Carmichael, "Quantum trajectory simulations of two-state behavior in an optical cavity containing one atom," Phys. Rev. A **46**, R6801–R6804 (1992).
2. W. Leoński and R. Tanaś, "Possibility of producing the one-photon state in a kicked cavity with a nonlinear Kerr medium," Phys. Rev. A **49**, R20–R23 (1994).
3. A. Imamoğlu, H. Schmidt, G. Woods, and M. Deutsch, "Strongly interacting photons in a nonlinear cavity," Phys. Rev. Lett. **79**, 1467–1470 (1997).
4. K. M. Birnbaum, A. Boca, R. Miller, A. D. Boozer, T. E. Northup, and H. J. Kimble, "Photon blockade in an optical cavity with one trapped atom," Nature (London) **436**, 87–90 (2005).
5. K. Müller, A. Rundquist, K. A. Fischer, T. Sarmiento, K. G. Lagoudakis, Y. A. Kelaita, C. S. Muñoz, E. del Valle, F. P. Laussy, and J. Vučković, "Coherent generation of nonclassical light on chip via detuned photon blockade," Phys. Rev. Lett. **114**, 233601 (2015).
6. X. Gu, A. F. Kockum, A. Miranowicz, Y.-X. Liu, and F. Nori, "Microwave photonics with superconducting quantum circuits," Phys. Rep. **718–719**, 1–102 (2017).
7. V. Scarani, H. Bechmann-Pasquinucci, N. J. Cerf, M. Dušek, N. Lütkenhaus, and M. Peev, "The security of practical quantum key distribution," Rev. Mod. Phys. **81**, 1301–1350 (2009).
8. I. Buluta, S. Ashhab, and F. Nori, "Natural and artificial atoms for quantum computation," Rep. Prog. Phys. **74**, 104401 (2011).
9. T. Peyronel, O. Firstenberg, Q.-Y. Liang, S. Hofferberth, A. V. Gorshkov, T. Pohl, M. D. Lukin, and V. Vuletić, "Quantum nonlinear optics with single photons enabled by strongly interacting atoms," Nature (London) **488**, 57–60 (2012).

10. C. Lang, D. Bozyigit, C. Eichler, L. Steffen, J. M. Fink, A. A. Abdumalikov, M. Baur, S. Filipp, M. P. da Silva, A. Blais, and A. Wallraff, "Observation of resonant photon blockade at microwave frequencies using correlation function measurements," Phys. Rev. Lett. **106**, 243601 (2011).
11. A. J. Hoffman, S. J. Srinivasan, S. Schmidt, L. Spietz, J. Aumentado, H. E. Türeci, and A. A. Houck, "Dispersive photon blockade in a superconducting circuit," Phys. Rev. Lett. **107**, 053602 (2011).
12. A. Faraon, I. Fushman, D. Englund, N. Stoltz, P. Petroff, and J. Vučković, "Coherent generation of non-classical light on a chip via photon-induced tunnelling and blockade," Nat. Phys. **4**, 859–863 (2008).
13. S. Ferretti, L. C. Andreani, H. E. Türeci, and D. Gerace, "Photon correlations in a two-site nonlinear cavity system under coherent drive and dissipation," Phys. Rev. A **82**, 013841 (2010).
14. J.-Q. Liao and C. K. Law, "Correlated two-photon transport in a one-dimensional waveguide side-coupled to a nonlinear cavity," Phys. Rev. A **82**, 053836 (2010).
15. A. Miranowicz, M. Paprzycka, Y.-X. Liu, J. Bajer, and F. Nori, "Two-photon and three-photon blockades in driven nonlinear systems," Phys. Rev. A **87**, 023809 (2013).
16. P. Rabl, "Photon blockade effect in optomechanical systems," Phys. Rev. Lett. **107**, 063601 (2011).
17. A. Nunnenkamp, K. Børkje, and S. M. Girvin, "Single-photon optomechanics," Phys. Rev. Lett. **107**, 063602 (2011).
18. J.-Q. Liao and F. Nori, "Photon blockade in quadratically coupled optomechanical systems," Phys. Rev. A **88**, 023853 (2013).
19. H. Xie, G.-W. Lin, X. Chen, Z.-H. Chen, and X.-M. Lin, "Single-photon nonlinearities in a strongly driven optomechanical system with quadratic coupling," Phys. Rev. A **93**, 063860 (2016).
20. C. Zhai, R. Huang, B. Li, H. Jing, and L.-M. Kuang, "Mechanical engineering of photon blockades in a cavity optomechanical system," arXiv:1901.07654 (2019).
21. W. Leoński and A. Miranowicz, "Kerr nonlinear coupler and entanglement," J. Opt. B **6**, S37–S42 (2004).
22. A. Miranowicz and W. Leoński, "Two-mode optical state truncation and generation of maximally entangled states in pumped nonlinear couplers," J. Phys. B **39**, 1683–1700 (2006).
23. T. C. H. Liew and V. Savona, "Single photons from coupled quantum modes," Phys. Rev. Lett. **104**, 183601 (2010).
24. M. Bamba, A. Imamoğlu, I. Carusotto, and C. Ciuti, "Origin of strong photon antibunching in weakly nonlinear photonic molecules," Phys. Rev. A **83**, 021802(R) (2011).
25. A. Majumdar, M. Bajcsy, A. Rundquist, and J. Vučković, "Loss-enabled sub-Poissonian light generation in a bimodal nanocavity," Phys. Rev. Lett. **108**, 163601 (2012).
26. S. Ferretti, V. Savona, and D. Gerace, "Optimal antibunching in passive photonic devices based on coupled nonlinear resonators," New J. Phys. **15**, 025012 (2013).
27. P. Kómár, S. D. Bennett, K. Stannigel, S. J. M. Habraken, P. Rabl, P. Zoller, and M. D. Lukin, "Single-photon nonlinearities in two-mode optomechanics," Phys. Rev. A **87**, 013839 (2013).
28. V. Savona, "Unconventional photon blockade in coupled optomechanical systems," arXiv:1302.5937 (2013).
29. X.-W. Xu and Y.-J. Li, "Antibunching photons in a cavity coupled to an optomechanical system," J. Phys. B **46**, 035502 (2013).
30. X.-W. Xu and Y. Li, "Strong photon antibunching of symmetric and antisymmetric modes in weakly nonlinear photonic molecules," Phys. Rev. A **90**, 033809 (2014).
31. W. Zhang, Z. Y. Yu, Y. M. Liu, and Y. W. Peng, "Optimal photon antibunching in a quantum-dot-bimodal-cavity system," Phys. Rev. A **89**, 043832 (2014).
32. H. Z. Shen, Y. H. Zhou, and X. X. Yi, "Tunable photon blockade in coupled semiconductor cavities," Phys. Rev. A **91**, 063808 (2015).
33. H. Flayac and V. Savona, "Unconventional photon blockade," Phys. Rev. A **96**, 053810 (2017).
34. H. Flayac and V. Savona, "Nonclassical statistics from a polaritonic Josephson junction," Phys. Rev. A **95**, 043838 (2017).
35. F. Zhou, D.-G. Lai, and J.-Q. Liao, "Photon blockade effect in a coupled cavity system," arXiv:1803.06642 (2018).
36. H. J. Snijders, J. A. Frey, J. Norman, H. Flayac, V. Savona, A. C. Gossard, J. E. Bowers, M. P. van Exter, D. Bouwmeester, and W. Löffler, "Observation of the unconventional photon blockade," Phys. Rev. Lett. **121**, 043601 (2018).
37. C. Vaneph, A. Morvan, G. Aiello, M. Féchant, M. Aprili, J. Gabelli, and J. Estève, "Observation of the unconventional photon blockade in the microwave domain," Phys. Rev. Lett. **121**, 043602 (2018).
38. A. Miranowicz, W. Leoński, and N. Imoto, "Quantum-optical states in finite-dimensional Hilbert space. I. General formalism," in *Modern Nonlinear Optics* (Wiley, 2001), Vol. **119**, pp. 195–213.
39. W. Leoński and A. Miranowicz, "Quantum-optical states in finite-dimensional Hilbert space. II. State generation," Adv. Chem. Phys. **119**, 155–193 (2003).
40. I. Carusotto and C. Ciuti, "Quantum fluids of light," Rev. Mod. Phys. **85**, 299–366 (2013).
41. S. Manipatruni, J. T. Robinson, and M. Lipson, "Optical nonreciprocity in optomechanical structures," Phys. Rev. Lett. **102**, 213903 (2009).
42. Z. Shen, Y.-L. Zhang, Y. Chen, C.-L. Zou, Y.-F. Xiao, X.-B. Zou, F.-W. Sun, G.-C. Guo, and C.-H. Dong, "Experimental realization of optomechanically induced non-reciprocity," Nat. Photonics **10**, 657–661 (2016).
43. N. R. Bernier, L. D. Tóth, A. Koottandavida, M. A. Ioannou, D. Malz, A. Nunnenkamp, A. K. Feofanov, and T. J. Kippenberg, "Nonreciprocal reconfigurable microwave optomechanical circuit," Nat. Commun. **8**, 604 (2017).
44. Q.-T. Cao, H. Wang, C.-H. Dong, H. Jing, R.-S. Liu, X. Chen, L. Ge, Q. Gong, and Y.-F. Xiao, "Experimental demonstration of spontaneous chirality in a nonlinear microresonator," Phys. Rev. Lett. **118**, 033907 (2017).
45. L. D. Bino, J. M. Silver, M. T. M. Woodley, S. L. Stebbings, X. Zhao, and P. Del'Haye, "Microresonator isolators and circulators based on the intrinsic nonreciprocity of the Kerr effect," Optica **5**, 279–282 (2018).
46. Y. Shi, Z. Yu, and S. Fan, "Limitations of nonlinear optical isolators due to dynamic reciprocity," Nat. Photonics **9**, 388–392 (2015).
47. L. Fan, J. Wang, L. T. Varghese, H. Shen, B. Niu, Y. Xuan, A. M. Weiner, and M. Qi, "An all-silicon passive optical diode," Science **335**, 447–450 (2012).
48. S. Zhang, Y. Hu, G. Lin, Y. Niu, K. Xia, J. Gong, and S. Gong, "Thermal-motion-induced non-reciprocal quantum optical system," Nat. Photonics **12**, 744–748 (2018).
49. K. Y. Xia, F. Nori, and M. Xiao, "Cavity-free optical isolators and circulators using a chiral cross-Kerr nonlinearity," Phys. Rev. Lett. **121**, 203602 (2018).
50. D. L. Sounas and A. Alù, "Non-reciprocal photonics based on time modulation," Nat. Photonics **11**, 774–783 (2017).
51. C. Caloz, A. Alù, S. Tretyakov, D. Sounas, K. Achouri, and Z.-L. Deck-Léger, "Electromagnetic nonreciprocity," Phys. Rev. Appl. **10**, 047001 (2018).
52. N. Bender, S. Factor, J. D. Bodyfelt, H. Ramezani, D. N. Christodoulides, F. M. Ellis, and T. Kottos, "Observation of asymmetric transport in structures with active nonlinearities," Phys. Rev. Lett. **110**, 234101 (2013).
53. B. Peng, S. K. Özdemir, F. Lei, F. Monifi, M. Gianfreda, G. L. Long, S. Fan, F. Nori, C. M. Bender, and L. Yang, "Parity-time-symmetric whispering-gallery microcavities," Nat. Phys. **10**, 394–398 (2014).
54. L. Chang, X. Jiang, S. Hua, C. Yang, J. Wen, L. Jiang, G. Li, G. Wang, and M. Xiao, "Parity-time symmetry and variable optical isolation in active-passive-coupled microresonators," Nat. Photonics **8**, 524–529 (2014).
55. S. Maayani, R. Dahan, Y. Kligerman, E. Moses, A. U. Hassan, H. Jing, F. Nori, D. N. Christodoulides, and T. Carmon, "Flying couplers above spinning resonators generate irreversible refraction," Nature (London) **558**, 569–572 (2018).
56. H. Lü, Y. Jiang, Y. Z. Wang, and H. Jing, "Optomechanically induced transparency in a spinning resonator," Photon. Res. **5**, 367–371 (2017).
57. H. Jing, H. Lü, S. K. Özdemir, T. Carmon, and F. Nori, "Nanoparticle sensing with a spinning resonator," Optica **5**, 1424–1430 (2018).

58. K. Y. Xia, G. W. Lu, G. W. Lin, Y. Q. Cheng, Y. P. Niu, S. Q. Gong, and J. Twamley, "Reversible nonmagnetic single-photon isolation using unbalanced quantum coupling," Phys. Rev. A **90**, 043802 (2014).
59. L. Tang, J. S. Tang, W. D. Zhang, G. W. Lu, Y. Zhang, K. Y. Xia, and M. Xiao, "An on-chip chiral single-photon interface: isolation and unidirectional emission," arXiv:1811.02957 (2018).
60. M. Scheucher, A. Hilico, E. Will, J. Volz, and A. Rauschenbeutel, "Quantum optical circulator controlled by a single chirally coupled atom," Science **354**, 1577–1580 (2016).
61. B. Abdo, K. Sliwa, S. Shankar, M. Hatridge, L. Frunzio, R. Schoelkopf, and M. Devoret, "Josephson directional amplifier for quantum measurement of superconducting circuits," Phys. Rev. Lett. **112**, 167701 (2014).
62. A. Metelmann and A. A. Clerk, "Nonreciprocal photon transmission and amplification via reservoir engineering," Phys. Rev. X **5**, 021025 (2015).
63. D. Malz, L. D. Tóth, N. R. Bernier, A. K. Feofanov, T. J. Kippenberg, and A. Nunnenkamp, "Quantum-limited directional amplifiers with optomechanics," Phys. Rev. Lett. **120**, 023601 (2018).
64. Z. Shen, Y.-L. Zhang, Y. Chen, F.-W. Sun, X. B. Zou, G. C. Guo, C.-L. Zou, and C. H. Dong, "Reconfigurable optomechanical circulator and directional amplifier," Nat. Commun. **9**, 1797 (2018).
65. A. Y. Song, Y. Shi, Q. Lin, and S. Fan, "Direction-dependent parity-time phase transition and non-reciprocal directional amplification with dynamic gain–loss modulation," Phys. Rev. A **99**, 013824 (2019).
66. S. Barzanjeh, M. Aquilina, and A. Xuereb, "Manipulating the flow of thermal noise in quantum devices," Phys. Rev. Lett. **120**, 060601 (2018).
67. R. Huang, A. Miranowicz, J.-Q. Liao, F. Nori, and H. Jing, "Nonreciprocal photon blockade," Phys. Rev. Lett. **121**, 153601 (2018).
68. X.-W. Xu, Y.-J. Zhao, H. Wang, H. Jing, and A.-X. Chen, "Nonreciprocal photon blockade via quadratic optomechanical coupling," arXiv:1809.07596 (2018).
69. P. Lodahl, S. Mahmoodian, S. Stobbe, A. Rauschenbeutel, P. Schneeweiss, J. Volz, H. Pichler, and P. Zoller, "Chiral quantum optics," Nature **541**, 473–480 (2017).
70. V. V. Konotop, J. K. Yang, and D. A. Zezyulin, "Nonlinear waves in PT-symmetric systems," Rev. Mod. Phys. **88**, 035002 (2016).
71. R. El-Ganainy, K. G. Makris, M. Khajavikhan, Z. H. Musslimani, S. Rotter, and D. N. Christodoulides, "Non-Hermitian physics and PT symmetry," Nat. Phys. **14**, 11–19 (2018).
72. J. Zhang, B. Peng, S. K. Özdemir, K. Pichler, D. O. Krimer, G. M. Zhao, F. Nori, Y.-X. Liu, S. Rotter, and L. Yang, "A phonon laser operating at an exceptional point," Nat. Photonics **12**, 479–484 (2018).
73. I. S. Grudinin, H. Lee, O. Painter, and K. J. Vahala, "Phonon laser action in a tunable two-level system," Phys. Rev. Lett. **104**, 083901 (2010).
74. H. Jing, S. K. Özdemir, X.-Y. Lü, J. Zhang, L. Yang, and F. Nori, "PT-symmetric phonon laser," Phys. Rev. Lett. **113**, 053604 (2014).
75. H. Lü, S. K. Özdemir, L.-M. Kuang, F. Nori, and H. Jing, "Exceptional points in random-defect phonon lasers," Phys. Rev. Appl. **8**, 044020 (2017).
76. Y. Jiang, S. Maayani, T. Carmon, F. Nori, and H. Jing, "Nonreciprocal phonon laser," Phys. Rev. Appl. **10**, 064037 (2018).
77. H. Zhang, F. Saif, Y. Jiao, and H. Jing, "Loss-induced transparency in optomechanics," Opt. Express **26**, 25199–25210 (2018).
78. Z.-P. Liu, J. Zhang, S. K. Özdemir, B. Peng, H. Jing, X.-Y. Lü, C.-W. Li, L. Yang, F. Nori, and Y.-X. Liu, "Metrology with PT-symmetric cavities: enhanced sensitivity near the PT-phase transition," Phys. Rev. Lett. **117**, 110802 (2016).
79. S. M. Spillane, T. J. Kippenberg, O. J. Painter, and K. J. Vahala, "Ideality in a fiber-taper-coupled microresonator system for application to cavity quantum electrodynamics," Phys. Rev. Lett. **91**, 043902 (2003).
80. H. Schmidt and A. Imamoğlu, "Giant Kerr nonlinearities obtained by electromagnetically induced transparency," Opt. Lett. **21**, 1936–1938 (1996).
81. Y.-P. Wang, G.-Q. Zhang, D. Zhang, T.-F. Li, C.-M. Hu, and J. Q. You, "Bistability of cavity magnon polaritons," Phys. Rev. Lett. **120**, 057202 (2018).
82. Z. R. Gong, H. Ian, Y.-X. Liu, C. P. Sun, and F. Nori, "Effective Hamiltonian approach to the Kerr nonlinearity in an optomechanical system," Phys. Rev. A **80**, 065801 (2009).
83. L. Ding, C. Baker, P. Senellart, A. Lemaitre, S. Ducci, G. Leo, and I. Favero, "Wavelength-sized GaAs optomechanical resonators with gigahertz frequency," Appl. Phys. Lett. **98**, 113108 (2011).
84. H. Snijders, J. A. Frey, J. Norman, M. P. Bakker, E. C. Langman, A. Gossard, J. E. Bowers, M. P. Van Exter, D. Bouwmeester, and W. Löffler, "Purification of a single-photon nonlinearity," Nat. Commun. **7**, 12578 (2016).
85. G. Enzian, M. Szczykulska, J. Silver, L. Del Bino, S. Zhang, I. A. Walmsley, P. Del'Haye, and M. R. Vanner, "Observation of Brillouin optomechanical strong coupling with an 11 GHz mechanical mode," Optica **6**, 7–14 (2019).
86. G. B. Malykin, "The Sagnac effect: correct and incorrect explanations," Phys. Usp. **43**, 1229–1252 (2000).
87. G. W. Ford, J. T. Lewis, and R. F. O'Connell, "Quantum Langevin equation," Phys. Rev. A **37**, 4419–4428 (1988).
88. C. W. Gardiner and P. Zoller, *Quantum Noise* (Springer, 2000).
89. D. F. Walls and G. J. Milburn, *Quantum Optics* (Springer, 1994).
90. J. R. Johansson, P. D. Nation, and F. Nori, "Qutip 2: a Python framework for the dynamics of open quantum systems," Comput. Phys. Commun. **184**, 1234–1240 (2013).
91. E. Verhagen, S. Deléglise, S. Weis, A. Schliesser, and T. J. Kippenberg, "Quantum-coherent coupling of a mechanical oscillator to an optical cavity mode," Nature (London) **482**, 63–67 (2012).
92. M. Aspelmeyer, T. J. Kippenberg, and F. Marquardt, "Cavity optomechanics," Rev. Mod. Phys. **86**, 1391–1452 (2014).
93. J. D. Teufel, T. Donner, D. Li, J. W. Harlow, M. S. Allman, K. Cicak, A. J. Sirois, J. D. Whittaker, K. W. Lehnert, and R. W. Simmonds, "Sideband cooling of micromechanical motion to the quantum ground state," Nature (London) **475**, 359–363 (2011).
94. K. J. Vahala, "Optical microcavities," Nature (London) **424**, 839–846 (2003).
95. V. Huet, A. Rasoloniaina, P. Guillemé, P. Rochard, P. Féron, M. Mortier, A. Levenson, K. Bencheikh, A. Yacomotti, and Y. Dumeige, "Millisecond photon lifetime in a slow-light microcavity," Phys. Rev. Lett. **116**, 133902 (2016).
96. J. Hloušek, M. Dudka, I. Straka, and M. Ježek, "Accurate detection of arbitrary photon statistics," arXiv:1812.02262 (2018).
97. R. Reimann, M. Doderer, E. Hebestreit, R. Diehl, M. Frimmer, D. Windey, F. Tebbenjohanns, and L. Novotny, "GHz rotation of an optically trapped nanoparticle in vacuum," Phys. Rev. Lett. **121**, 033602 (2018).
98. J. Ahn, Z. Xu, J. Bang, Y.-H. Deng, T. M. Hoang, Q. Han, R.-M. Ma, and T. Li, "Optically levitated nanodumbbell torsion balance and GHz nanomechanical rotor," Phys. Rev. Lett. **121**, 033603 (2018).
99. F. Reiter, T. L. Nguyen, J. P. Home, and S. F. Yelin, "Cooperative breakdown of the oscillator blockade in the Dicke model," arXiv:1807.06026 (2018).
100. M. Radulaski, K. A. Fischer, K. G. Lagoudakis, J. L. Zhang, and J. Vučković, "Photon blockade in two-emitter-cavity systems," Phys. Rev. A **96**, 011801(R) (2017).
101. M. B. Plenio and P. L. Knight, "The quantum-jump approach to dissipative dynamics in quantum optics," Rev. Mod. Phys. **70**, 101–144 (1998).